European Review for Medical and Pharmacological Sciences 2020; 24: 6494-6504

MiR-205-3p protects human corneal epithelial cells from ultraviolet damage by inhibiting autophagy *via* targeting TLR4/NF-κB signaling

J.-Y. FU[1], X.-F. YU[1], H.-Q. WANG[1], J.-W. LAN[1], W.-Q. SHAO[1], Y.-N. HUO[2]

[1]Ophthalmology Department, Second People's Hospital of Quzhou, Quzhou, China
[2]Eye Center, Second Affiliated Hospital of Zhejiang University School of Medicine, Hangzhou, China

Abstract. – OBJECTIVE: MiRNA has been found to have therapeutic effect on corneal damage. This paper aimed to study the effect of miR-205-3p on corneal damage induced by ultraviolet (UV) radiation.

MATERIALS AND METHODS: HCE cell were exposed to UV light and transfected. Quantitative Real Time-Polymerase Chain Reaction (qRT-PCR) and Western blot were used to determine miRNA/mRNA and protein expression. CCK-8 assay, Edu incorporation experiment, and flow cytometry were used to separately measure cell activity, proliferation and apoptosis. LC3 puncta were researched by immunofluorescence experiment. TNF-α, IL-6 and IL-1β levels in cells were detected by enzyme-linked immunosorbent assay (ELISA) kit. MDA, SOD, and GSH-PX levels were measured using detection kits. Reactive oxygen species (ROS) level was reflected by detecting DCFH-DA density. Luciferase activity assay was performed to verify the regulating relationship between miR-205-3p and TLR4.

RESULTS: UV radiation decreased HCE cell viability, proliferation, and increased HCE cell apoptosis and autophagy (all $p < 0.01$). When exposed UV radiation, the overexpression of miR-205-3p group elevated HCE cells viability, proliferation and weakened HCE cells apoptosis and autophagy (all $p < 0.01$). MiR-205-3p inhibited inflammation and oxidative stress in HCE cells induced by UV radiation ($p < 0.01$). MiR-205-3p directly inhibited TLR4 expression. The upregulation of TLR4 significantly reversed the effects of miR-205-3p on HCE cell phenotypes induced by UV radiation ($p < 0.01$).

CONCLUSIONS: MiR-205-3p protected HCE cells from UV damage by inhibiting autophagy via targeting TLR4.

Key Words:
Corneal damage, Ultraviolet (UV), MiR-205-3p, Autophagy, TLR4.

Introduction

Ultraviolet (UV) radiation is a major cause of eye damage[1]. It has been observed that free radicals (such as oxygen-derived free radicals) could be generated by UV radiation and these free radicals could result in the lipid peroxidation in the cell membrane[2]. UV radiation was also proved to directly cause DNA damage, which led to apoptosis, autophagy and inflammation, reduced mitochondrial function and destroyed ocular structures, such as cornea, retina, and lens[2,3]. As one of the important structures of eye, the corneal epithelium has the physiological function of absorbing most of the environmental UV radiation. As a result, the sub-corneal tissues of corneal epithelium, the lens and retina are protected from UV radiation[4].

MicroRNA (miRNA) is a short-chain non-coding RNA of 20-22 nucleotides in length[5]. Existing researches discovered the therapeutic value of miRNA for corneal damage. Corneal scarring caused by corneal damage was one of the main causes of vision loss. Ratuszny et al[6] illustrated that miR-145 might be a promising target to prevent the formation of cornea scarring. MiR-204 expression was discovered to be significantly decreased during the healing of mouse corneal epithelial wound. The declined expression of miR-204 promoted the proliferation and migration of human corneal epithelial cells. MiR-204 was thus considered to be a biomarker for the healing process of corneal injury[7]. In the model of corneal damage caused by alkali burns, miR-466 suppressed lymphangiogenesis *via* regulating prospero-related homeobox 1[8]. Moreover, within 24 h after scratch injury of human and mouse corneal epithelial cells, the expression of miR-

Corresponding Author: Yanan Huo, MD; e-mail: 3309035@zju.edu.cn

205 was significantly elevated. Notably, the use of miR-205 antagomer prominently delayed the regrowth of the injured human corneal epithelial cells[9].

However, at present, research on miRNA in corneal damage caused by UV radiation is still rarely to see. Since miR-205 was found to be involved in the regulation of corneal injury, the present research was aimed to further investigate the effect of miR-205-3p on corneal damage caused by UV radiation. We noticed from previous studies[10-12] that miR-205 could impair the autophagic flux and regulate radiosensitivity by suppressing autophagy of human tumor cells. Therefore, we speculated that miR-205-3p might be involved in the healing of corneal damage caused by UV radiation *via* regulating autophagy. To the best of our knowledge, this was the first study to research the role of miR-205-3p in the healing of corneal damage caused by UV radiation.

Materials and Methods

Ethics Committee

This study has been approved by Ethics Committee of the Second People's Hospital of Quzhou, China.

Cell Line

Human corneal epithelial cell line (HCE) was obtained from the Shanghai Institute of Cell Biology, Chinese Academy of Sciences (Shanghai, China). The cells were cultured in Dulbecco's Modified Eagle's Medium (DMEM) containing 10% fetal bovine serum (FBS) in a sterile 25 cm^2 culture flask at 37°C, 5% CO_2. The culture medium was changed every three days and cells were passaged three times.

Exposure of HCE Cells to UV Light

HCE cells were collected at a confluency of 80%. Phosphate buffer saline (PBS, 1 mL) was used to disperse cells. The cells dispersed in PBS were transferred to a 60 mm petri dish for 3 h radiation with an ultraviolet B (UVB) lamp. The vertical distance from the UVB lamp to the petri dish was 12 cm. The wavelength range was 250-350 nm with a peak wavelength of 297 nm. The UV radiation intensity was 20 μw/cm^2. After 3 h radiation[2], cells were re-suspended in a culture flask with 5 mL DMEM containing 10% FBS at 37°C, 5% CO_2.

Transfection and Group

HCE cells without any treatment were served as Con group. Those cells irradiated with UVB lamp for 3 h were set as UV group. Cells of the two groups were dispersed in DMEM containing 10% FBS and then seeded in 6-well plates with $1*10^5$ cells per well.

In addition, HCE cells irradiated with UVB lamp were cultured in DMEM without FBS for 24 h. Then, they were subjected to transfection with miR-205-3p mimics (UV + miR-205-3p group) and corresponding negative control (UV + miR-NC group). Moreover, HCE cells irradiated with UVB lamp were also co-transfected with miR-205-3p mimics and pcDNA3.1-TLR4 overexpression vector (UV + miR-205-3p + TLR4 group). MiR-205-3p mimics, negative control and pcDNA3.1-TLR4 overexpression vector were all provided by Jima Pharmaceutical Technology (Shanghai, China). Lipofectamine 2000 reagent (Thermo Fisher Scientific, Waltham, MA, USA) was used for transfection. HCE cells of the three groups were collected after 8 h of transfection, followed by being inoculated in 6-well plates with $1 * 10^5$ cells and 1 mL DMEM (10% FBS) per well. At last, all the cells of the above five groups were maintained at 37°C, 5% CO_2 for 48 h.

Quantitative Real Time-Polymerase Chain Reaction (qRT-PCR)

According to the instructions, total RNA in HCE cells were extracted with TRIzol reagent (Life Technologies, Foster City, CA, USA). The cDNA templates were synthesized with using PrimeScript RT reagent Kit (TaKaRa Bio, Otsu, Shiga, Japan). By using the SYBR Premix Ex Taq II (Takara Bio, Otsu, Shiga, Japan) with an ABI 7500 Sequence Detection System (Applied Biosystems, Foster City, CA, USA), the qRT-PCR for miR-205-5p and TLR4 mRNA were conducted. U6 was set as the endogenous control for miR-205-5p while GAPDH was served as the internal control for TLR4 mRNA. The primer sequences were listed as follows: miR-205-5p, forward, 5'-TCCACCGGAGTCTGTCTCAT-3', reverse, 5'-GCTGTCAACGATACGCTACG-3'. U6, forward, 5'-CTCGCTTCGGCAGCACATATACT-3', reverse, 5'-ACGCTTCACGAATTTGCGTGTC-3'. TLR4, forward, 5'-GCTTTCACCTCTGCCTTCAC-3', reverse, 5'-AGGCGATACAATTCCACCTG-3'. GAPDH, forward, 5'-GTCGATGGCTAGTCGTAGCATCGAT-3', reverse, 5'-TGCTAGCTGGCATGCCCGATCGATC-3'. The amplification condition was as follows: 95°C

for 10 min, and 40 cycles of 95°C for 20 s, 60°C for 30 s and 72°C for 30 s. The relative expression of miR-205-5p and TLR4 mRNA was calculated with the $2^{-\Delta\Delta CT}$ method.

Cell Counting Kit-8 (CCK-8) Assay

HCE cells of each group were collected at about 80% confluency. DMEM (10% FBS) was used to prepare cell suspensions with a density of $1*10^5$ cells/mL. Each cell suspension sample was added into 96-well plates (100 μL per well). Five duplicate wells were set. All the plates were maintained in the incubator at 37°C, 5% CO_2 for 72 h. After that, all the plates were removed out from the incubator. Subsequently, 10 μL CCK-8 solutions were added into each well for 2 h incubation at 37°C. The optical density (OD) value of each well was measured at a wavelength of 450 nm (OD450 value). The OD450 value of wells containing 100 μL DMEM (10% FBS) and 10 μL CCK-8 solution was used as the blank. Cell viability of each well was calculated as follows: the OD450 value of each well/the OD450 value of the blank.

5-Ethynyl-2-Deoxy-Uridine (Edu) Incorporation Experiment

Edu incorporation experiment was performed with EdU assay kit (Ribobio, Guangzhou, China) to intuitively observe cells proliferative. According to the instructions, the cells cultured in DMEM (10% FBS) at 37°C, 5% CO_2 were treated with 40 μmol/L EdU for 2 h. Formaldehyde (4%) was used to fix cells, and then, the cells were treated with 0.5% Triton X100. Reaction cocktail was added into these cells for 30 min incubation at room temperature in darkness. After the nucleus was counterstained with 4'-6-diamidino-2-phenylindole (DAPI), the number of Edu positive cell number (red fluorescence) was counted in 5 random × 400 magnification fields under a fluorescence microscope. Greater Edu positive cell number indicated stronger cell proliferation ability.

Apoptosis Analysis

Flow cytometry assay was carried out to display cell apoptosis more accurately. Briefly, HCE cells of each group were harvested after 48 h incubation and washed with PBS for three times. Then, annexin V-fluorescein isothiocyanate (Annexin V-FITC) and propidium iodide (PI) was added into cells for 15 min incubation in the dark. With a flow cytometer (Beckman-Coulter, Fullerton, CA, USA), cells apoptosis rate was detected. For cells of each group, the apoptosis rate was tested independently at least three times.

Immunofluorescence Experiment

Immunofluorescence experiment was performed to detect the puncta of LC3 in HCE cells. In short, HCE cells of each group were seeded in 6-well plates with a density of $1*10^5$ cells per well. Notably, a glass coverslip was placed in advance at the bottom of each well. A total of 1 mL DMEM (10% FBS) was contained in each well. Cells were cultured at 37°C, 5% CO_2 until attached to the glass coverslip. Then, 4% paraformaldehyde was used to fix cells for 10 min. Subsequently, 0.3% Triton X-100 was added into cells for permeabilization. Cells were sequentially incubated with LC3 primary antibody and Alexa Fluor 488-conjugated secondary antibody. The primary antibody and secondary antibody used in this section were provided by Invitrogen (Carlsbad, CA, USA). The nucleus was stained with DAPI. Cells were observed under a confocal microscopy (Olympus Corp., Tokyo, Japan) and the LC3 puncta (red fluorescence) was counted[13].

Western Blot

Radioimmunoprecipitation assay (RIPA) cell lysate and protease inhibitor was added into cells for 30 min incubation on ice. At 4°C, the cells were centrifuged for 30 min at 1200 r/min in order to obtain the supernatant. A total of 80 μg supernatant was underwent protein separation with 12% sodium dodecyl sulfate-polyacrylamide gel electrophoresis (SDS-PAGE). Protein was then transferred to a polyvinylidene difluoride (PVDF) membrane to perform 2 h blocking with 5% skimmed milk. Primary antibodies were respectively used to incubate the PVDF membrane at 4°C overnight, followed by incubation with horseradish peroxidase-conjugated goat anti-mouse or anit-rabbit secondary antibodies for 2 h at room temperature. The primary antibodies used in this research were as follows: rabbit polyclonal anti-LC3I (1:1000, Cell Signaling Technology, Beverly, MA, USA), rabbit polyclonal anti-LC3II (1:1000, Cell Signaling Technology, Beverly, MA, USA), rabbit anti-ATG5 (1:1000, Abcam, Cambridge, MA, USA), rabbit anti-P62 (1:1000, Abcam, Cambridge, MA, USA), rabbit anti-Berclin-1 (1:500, Abcam, Cambridge, MA, USA), mouse anti-GAPDH polyclonal antibody

(1:1000, Abcam, Cambridge, MA, USA), rabbit polyclonal anti-TLR4 (1:1000, Santa-Cruz Biotechnology, Santa Cruz, CA, USA), rabbit polyclonal anti-NF-κB (1:500, Cell Signaling Technology, Beverly, MA, USA), rabbit polyclonal anti-p-NF-κB (1:500, Santa-Cruz Biotechnology, Santa Cruz, CA, USA). After washing with Tris-Buffered Saline and Tween 20 (TBST), the PVDF membrane was incubated with enhanced chemiluminescence detection reagent (Thermo Fisher Scientific, Waltham, MA, USA). The blots were scanned by a Gel-doc2000 imaging system (Bio-Rad, Hercules, CA, USA). The optical density of each blot was analyzed with Quantity One 1-D Analysis software (Systat Software, San Jose, CA, USA).

Enzyme-Linked Immunosorbent Assay (ELISA)

After 48 h of culture, HCE cells of each group were harvested and washed three times with PBS. After being centrifuged for 5 min at 1000 r/min, the cells were incubated with PBS containing cell lysates for 10 min at 4°C. The supernatant was harvested after 5 min centrifugation at 12 000 r/min. The level of TNF-α, IL-6 and IL-1β in the supernatant was detected by using ELISA kit in strict accordance with the instructions.

Malonaldehyde (MDA), Superoxide Dismutase (SOD) and Glutathione Peroxidase (GSH-PX) Levels Detection

HCE cells were incubated for 48 h at 37°C, 5% CO_2, followed by washing with PBS and lysed with cell lysates. The supernatant was obtained by 5 min centrifugation at 12 000 r/min. The level of MDA, SOD and GSH-PX in each supernatant sample was determined using detection kits. All the kits used for MDA, SOD, and GSH-PX detection were provided by Boster (Wuhan, China).

Detection of Reactive Oxygen Species (ROS)

The level of intracellular ROS was assessed by the fluorescent dye dichloro-dihydro-fluorescein diacetate (DCFH-DA). In short, a total of $5*10^4$ HCE cells were seeded in 96-well plates for 48 h culture at 37°C, 5% CO_2. After washing with PBS, the cells were incubated with 10 μmol/L of DCFH-DA (Sigma-Aldrich, St Louis, MO, USA) for 30 min at 37°C in the darkness. The DCFH-DA density (green fluorescence) was determined by flow cytometer (Beckman-Coulter, Fullerton, CA, USA).

Luciferase Activity Assay

Human embryonic kidney cells (HEK293) were cultured in DMEM (10% FBS) and were sub-cultured three times. The third generation HEK293 cells were collected in the logarithmic growth phase. Then, the cells were dispersed in DMEM without PBS with a density of $1*10^5$ cells per well. The cell suspensions were inoculated in 6-well plates (1 mL per well) for 24 h culture at 37°C, 5% CO_2. MiR-205-3p mimics or negative control was transfected into HEK293 cells. TLR4 mutant type (MUT) and wild type (WT) fragments were designed and synthesized by Jima Pharmaceutical Technology (Shanghai, China). Luciferase reporter plasmids containing the TLR4-MUT-3'UTR or TLR4-WT-3'UTR were subsequently co-transfected into these HEK293 cells. Lipofectamine 2000 reagent (Thermo Fisher Scientific, Waltham, MA, USA) was used for transfection. After 48 h culture at 37°C, 5% CO_2, the Luciferase reporter activity of cells was determined by Dual-Luciferase Assay System (Promega Corporation, Madison, WI, USA).

Statistical Analysis

All data in this paper was expressed in the form of mean ± standard deviation (SD). Statistical significance between two groups was evaluated by Student's *t*-test. One-way analysis of variance was used to perform comparison at least three groups. Tukey's post-hoc test was used to validate ANOVA for pairwise comparisons. Statistical Program and Service Solution (SPSS) 19.0 software (SPSS Inc., Chicago, IL, USA) was used to process data. $p < 0.05$ was considered as statistical significant difference. All experiments in this paper were carried out independently at least three times.

Results

MiR-205-3p Enhanced HCE Cells Proliferation Induced by UV Radiation

The miR-205-3p expression in HCE cells was measured after UV radiation. Relative to HCE cells of Control group, those of UV group exhibited significantly decreased miR-205-3p expression ($p < 0.01$) (Figure 1A). After transfection, HCE cells viability, proliferation and apoptosis was respectively detected by CCK-8 assay, Edu experiment, and flow cytometry. As shown in Figure 1B, C, and D, HCE cells of UV group had

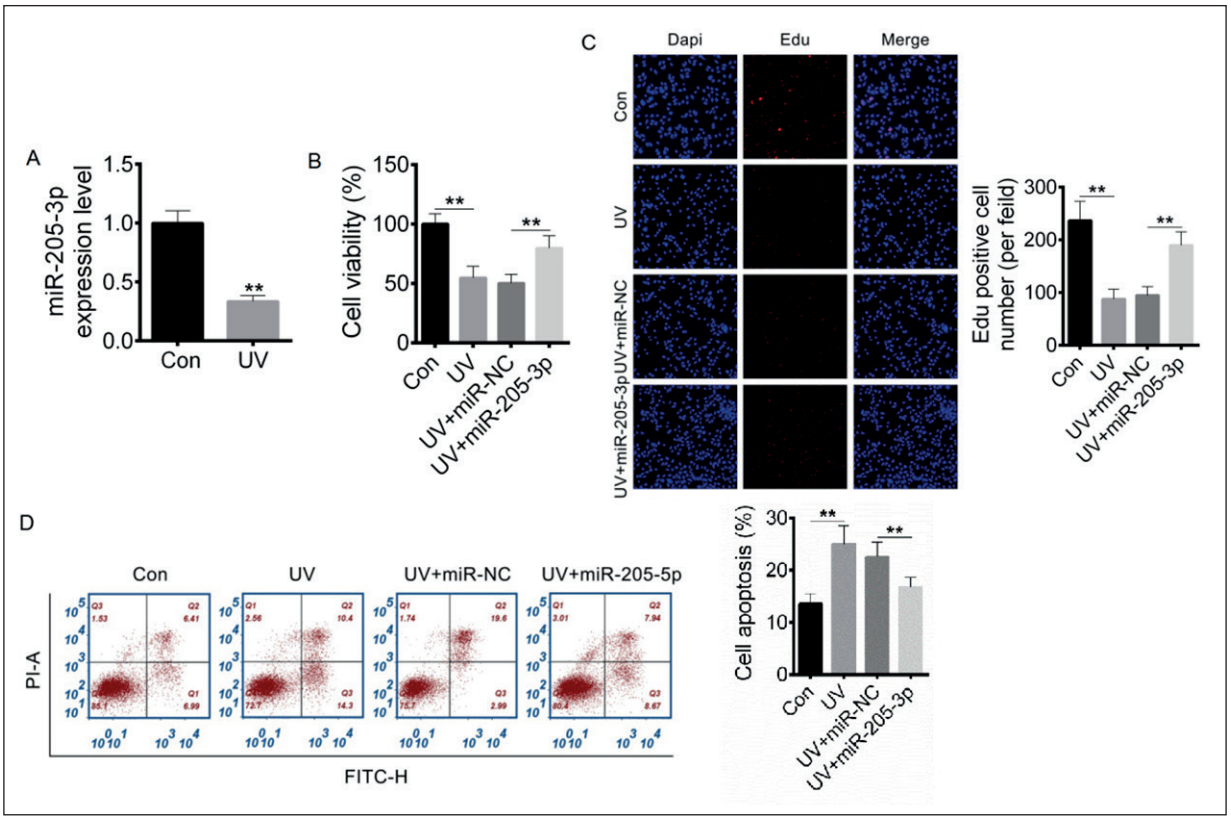

Figure 1. MiR-205-3p enhanced HCE cells proliferation induced by UV radiation. **A,** The miR-205-3p expression in HCE cells was measured by qRT-PCR after UV radiation. **B,** HCE cells viability was detected by CCK-8 assay. **C,** HCE cells proliferation was assessed by Edu experiment (magnification: × 400). **D,** HCE cells apoptosis was evaluated by flow cytometry. ** $p < 0.01$.

much lower cell viability ($p < 0.01$) and Edu positive cell number ($p < 0.01$), but higher apoptosis percentage ($p < 0.01$) than those of Con group. Notably, when compared with UV + miR-NC group, HCE cells of UV + miR-205-3p group showed markedly higher cell viability ($p < 0.01$) and Edu positive cell number ($p < 0.01$), but lower apoptosis percentage ($p < 0.01$).

MiR-205-3p Inhibited HCE Cells Autophagy Induced by UV Radiation

Immunofluorescence experiment was used to detect the puncta of LC3 in HCE cells. As shown in Figure 2A, the LC3 puncta of HCE cells in UV group was prominently higher than that of Con group ($p < 0.01$). Relative to UV + miR-NC group, HCE cells of UV + miR-205-3p group had significantly lower LC3 puncta ($p < 0.01$). Subsequently, the expression of autophagy-related proteins was assessed by Western blot. The results showed that, compared with Con group, HCE cells of UV group had markedly higher LC3II/I, ATG5 and Berclin-1 proteins expression ($p < 0.01$) and significantly lower P62 protein expression ($p < 0.01$). However, relative to UV + miR-NC group, much lower LC3II/I, ATG5 and Berclin-1 proteins expression ($p < 0.01$) and remarkably higher P62 protein expression ($p < 0.01$) were found in HCE cells of UV + miR-205-3p group ($p < 0.01$) (Figure 2B).

MiR-205-3p Inhibited Inflammation and Oxidative Stress in HCE Cells Induced by UV Radiation

The results from ELISA test illustrated much higher TNF-α, IL-6 and IL-1β level in HCE cells of UV group than that of Con group ($p < 0.01$). However, HCE cells of UV + miR-205-3p group exhibited significantly lower TNF-α, IL-6 and IL-1β level than that of UV + miR-NC group ($p < 0.01$) (Figure 3A, B, C). Furthermore, dramatically higher MAD level, lower SOD and GSH-PX levels was observed in HCE cells of UV group when compared with Con group ($p < 0.01$). Lower MAD level, higher SOD and GSH-PX level was occurred in HCE cells of UV + miR-205-3p

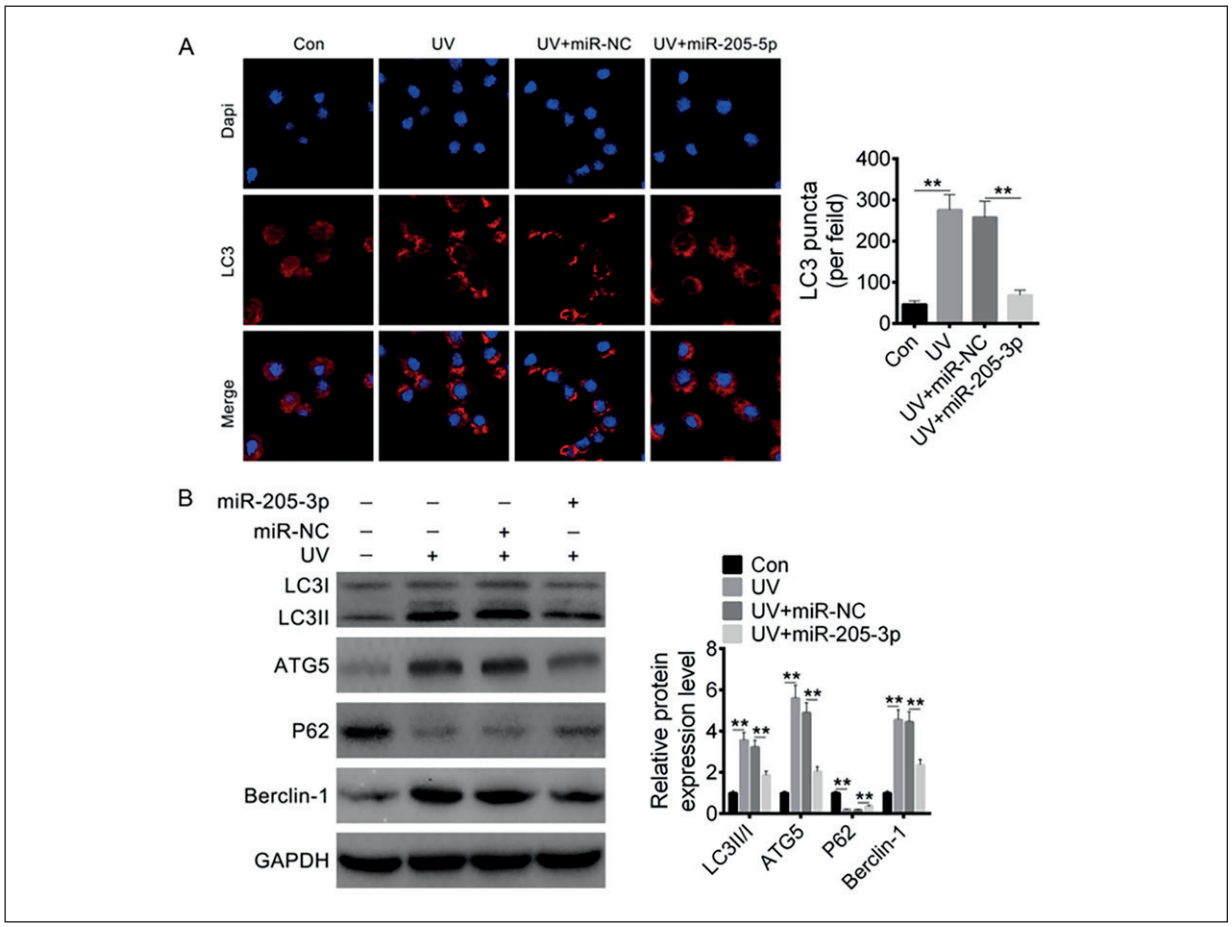

Figure 2. MiR-205-3p inhibited HCE cells autophagy induced by UV radiation. **A,** Immunofluorescence experiment was used to detect the puncta of LC3 in HCE cells (magnification: × 400). **B,** The expression of autophagy-related proteins in HCE cells was assessed by Western blot. ** $p < 0.01$.

group relative to UV + miR-NC group ($p < 0.01$) (Figure 3D, E, F). In addition, the ROS level was reflected by detecting intracellular fluorescence using flow cytometry. As shown in Figure 3G, compared with Con group, HCE cells of UV group showed much higher relative DCFH-DA density ($p < 0.01$). However, remarkably reduced relative DCFH-DA density was found in HCE cells of UV + miR-205-3p group when compared to UV + miR-NC group ($p < 0.01$).

MiR-205-3p Directly Inhibited the Expression of TLR4

Target Scan online prediction results showed that miR-205-3p possessed the binding site for TLR4 (Figure 4A). The results from the Luciferase activity assay revealed that, after the MUT-TLR4-3'UTR fragment being inserted, comparable relative Luciferase activity was found between miR-NC group and miR-205-3p group. However, by inserting WT-TLR4-3'UTR fragment, HEK293 cells of miR-205-3p group exhibited significantly lower relative Luciferase activity than miR-NC group ($p < 0.01$) (Figure 4B). Then, TLR4 mRNA and protein expression in HCE cells was determined by qRT-PCR and Western blot. HCE cells of UV group had much higher TLR4 mRNA and protein expression relative to Con group ($p < 0.01$). Notably, when compared with UV + miR-NC group, prominently lower TLR4 mRNA and protein expression was observed in HCE cells of UV + miR-205-3p group ($p < 0.01$) (Figure 4C, D).

MiR-205-3p Protected HCE Cells from UV Damage Via Regulating TLR4/NF-κB Signaling

HCE cells of UV + miR-205-3p group exhibited significantly higher cell viability and lower apoptosis percentage when compared with UV + miR-NC

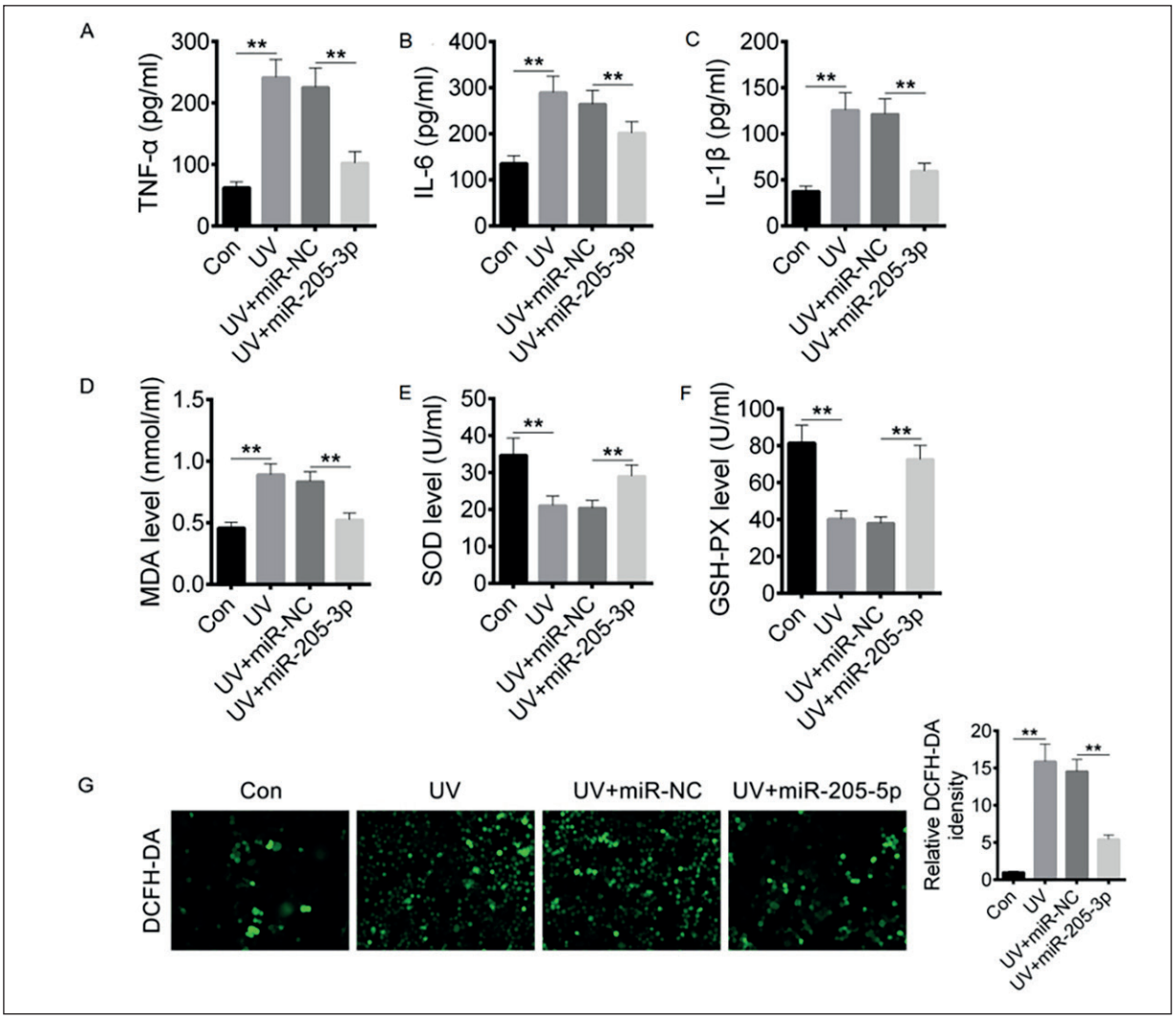

Figure 3. MiR-205-3p inhibited inflammation and oxidative stress in HCE cells induced by UV radiation. **A-B,** and **C,** TNF-α, IL-6, and IL-1β level in HCE cells was detected by ELISA test. **D-E,** and **F,** MAD, SOD and GSH-PX level in HCE cells was detected using the kit. **G,** The ROS level was reflected by detecting intracellular fluorescence using flow cytometry (magnification: × 200). ** $p < 0.01$.

group and UV + miR-205-3p + TLR4 group ($p < 0.01$) (Figure 5A, B). As shown in Figure 5C, the LC3 puncta of HCE cells in UV + miR-205-3p group was much lower than that in UV + miR-NC group and UV + miR-205-3p + TLR4 group ($p < 0.01$). In terms of inflammatory factors, HCE cells of UV + miR-205-3p group showed much lower TNF-α, IL-6 and IL-1β levels than UV + miR-NC group and UV + miR-205-3p + TLR4 group ($p < 0.01$) (Figure 5D, E, F). Meanwhile, much higher GSH-PX, SOD levels and lower MDA level was occurred in HCE cells of UV + miR-205-3p group relative to UV + miR-NC group and UV + miR-205-3p + TLR4 group ($p < 0.01$) (Figure 5G, H, I). ROS level detection indicated that, HCE cells of UV + miR-205-3p group had much lower relative DCFH-DA density than UV + miR-NC group and UV + miR-205-3p + TLR4 group ($p < 0.01$) (Figure 5J). In addition, prominently lower TLR4, p-NF-κB/NF-κB, LC3II/I, ATG5, Berclin-1 protein expression and higher P62 protein expression was observed in HCE cells of UV + miR-205-3p group when relative to UV + miR-NC group and UV + miR-205-3p + TLR4 group ($p < 0.01$) (Figure 5K).

Discussion

It has been discovered that radiation of cells by UV light could trigger various signaling cascades

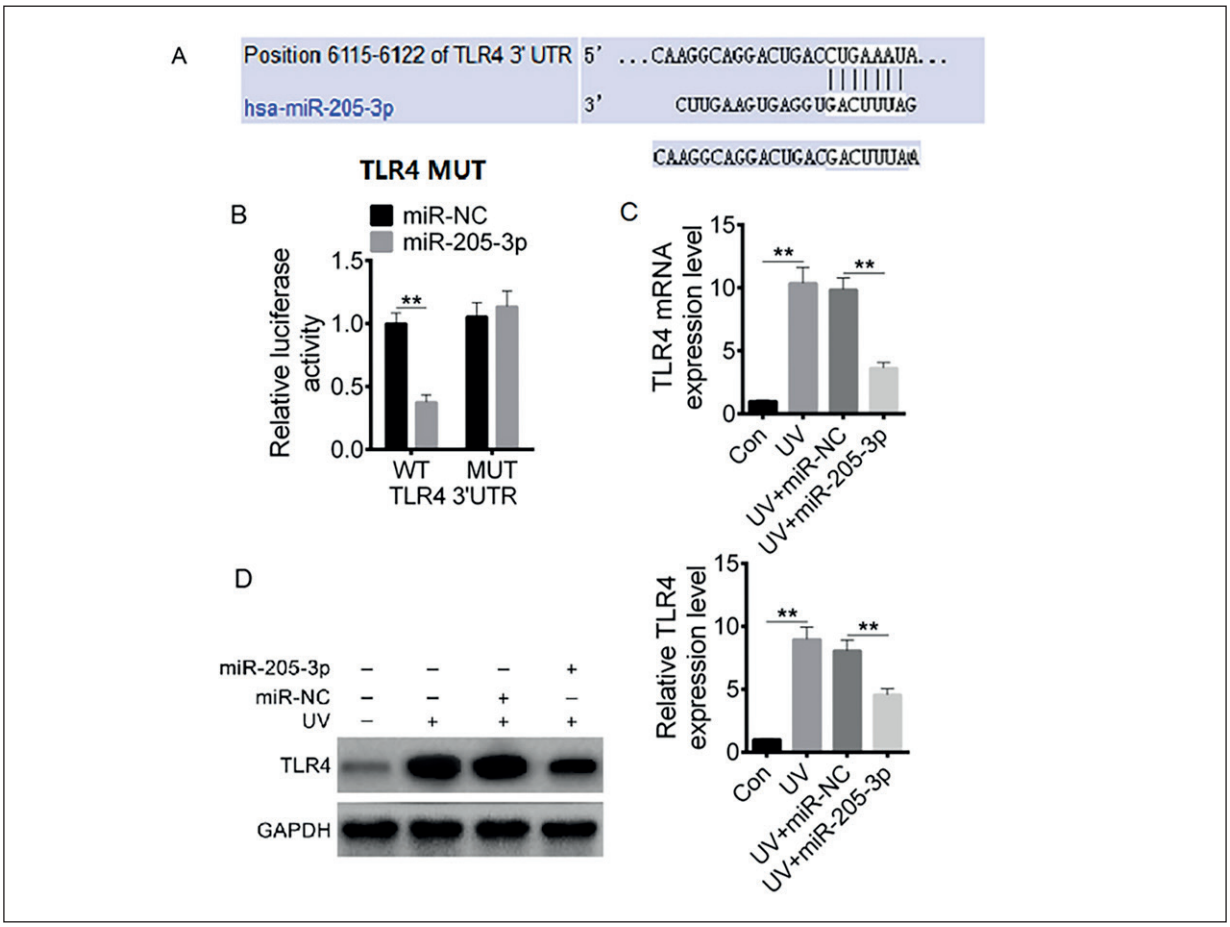

Figure 4. MiR-205-3p directly inhibited the expression of TLR4. **A,** Target Scan online prediction results showed that miR-205-3p possessed the binding site for TLR4. **B,** Luciferase activity assay was performed to verify the regulatory relationship between miR-205-3p and TLR4. **C,** TLR4 mRNA expression in HCE cells was determined by qRT-PCR. **D,** TLR4 protein expression in HCE cells was assessed by Western blot. ** $p < 0.01$.

and these signaling cascades ultimately promoted apoptosis of cells[14]. A large number of free radicals were generated in the corneal tissues after being exposed to UV light. As a result, biological tissues might be damaged if the insufficient supply of free radical scavengers was occurred in the irradiated tissues. Exposure to UV radiation could cause damage and even death of corneal epithelial cells, which was contributed to the development of ocular lesions such as photokeratitis[2]. The findings of this study indicated that exposure to UV radiation could result in HCE cells damage, such as reduced viability and proliferation, and enhanced apoptosis, autophagy, inflammatory response and oxidative stress. However, overexpression of miR-205-3p could protect HCE cells from UV damage. Mechanically, miR-205-3p might protect HCE cells from UV damage by inhibiting autophagy *via* targeting TLR4.

Several miRNAs have been discovered to be involved in the regulation of corneal damage. However, it is still difficult to find relevant literatures on miRNAs intervention in corneal damage caused by UV radiation. This study indicated for the first time that miR-205-3p upregulation could attenuate autophagy in HCE cells induced by UV radiation. To date, miR-205-3p is rarely researched in human diseases and tissue damage. In the existing literatures, miR-205-3p was only found to be overexpressed in non-small cell lung cancer[15]. In colorectal cancer cells exposed to low doses of ionizing radiation, the expression level of miR-205-3p was significantly increased, thereby increasing the radiosensitivity of colorectal cancer cells[16]. Our results proved for the first time that miR-205-3p protected HCE cells from UV damage by inhibiting autophagy.

Autophagy is a lysosomal degradation mechanism that is crucial for the physiological function

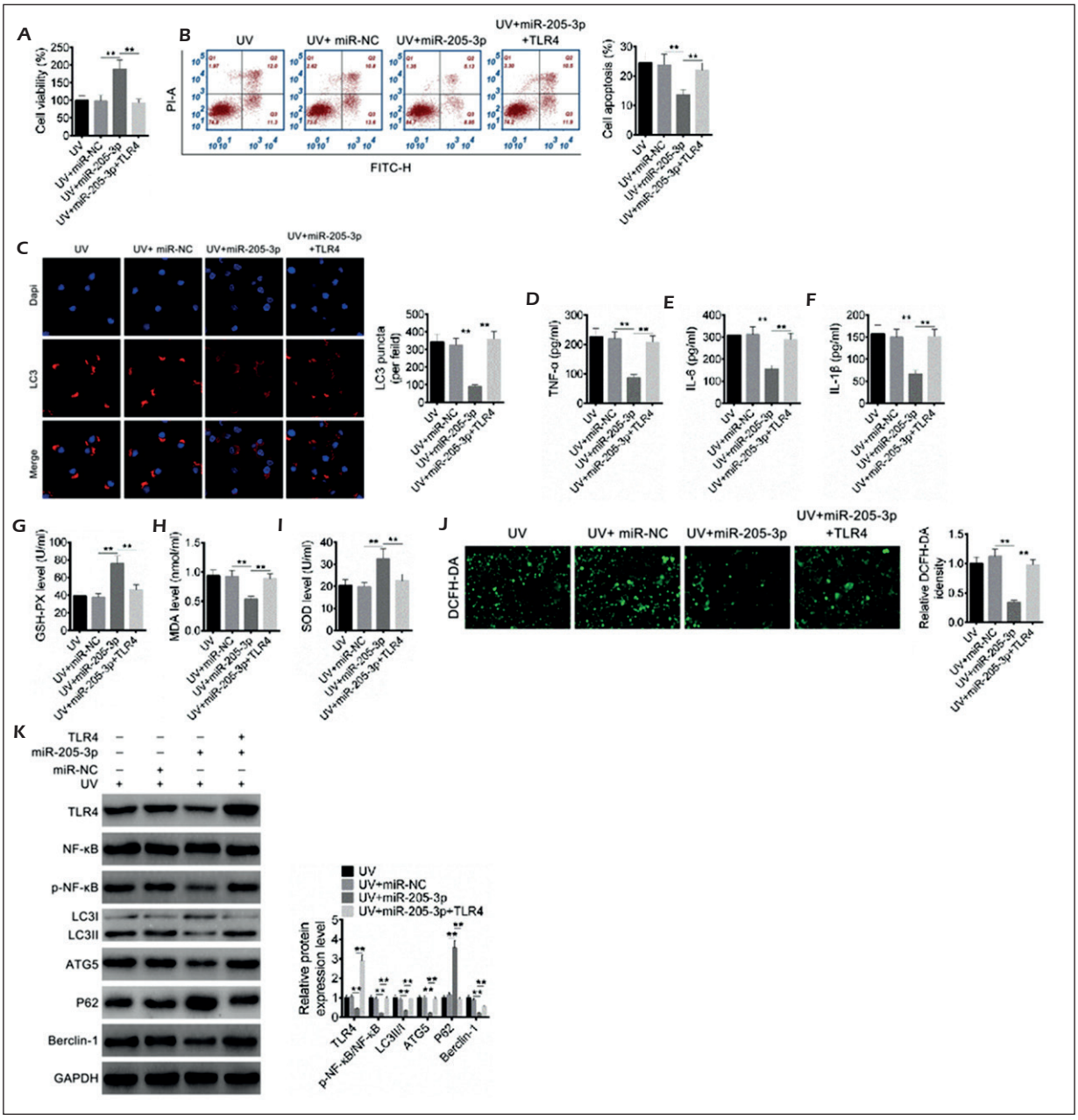

Figure 5. MiR-205-3p protected HCE cells from UV damage via regulating TLR4/NF-κB signaling. **A,** HCE cells viability was detected by CCK-8 assay. **B,** HCE cells apoptosis was evaluated by flow cytometry. **C,** Immunofluorescence experiment was used to detect the puncta of LC3 in HCE cells (magnification: × 400). **D-E,** and **F,** TNF-α, IL-6, and IL-1β level in HCE cells was detected by ELISA test. **G-H,** and **I,** MAD, SOD and GSH-PX level in HCE cells was detected using the kit. **J,** The ROS level was reflected by detecting intracellular fluorescence using flow cytometry (magnification: × 200). **K,** TLR4, p-NF-κB/NF-κB, LC3II/I, ATG5, Berclin-1 and P62 protein expression was assessed by Western blot. ** $p < 0.01$.

and stress defense of cells[17]. Maria et al[18] suggested that autophagic machinery was involved in the regulation of cell cycle in the limbal stem cells under UV radiation. Autophagy is also often found in other injuries or diseases caused by UV radiation. Qiang et al[19] illustrated that UV radiation induced autophagy in epidermal cells, leading to the occurrence of inflammation and skin tumorigenesis. Misovic et al[20] declared that UV radiation caused autophagy in human keratinocytes, and UV-induced apoptosis could be suppressed by intervention with autophagy. From

this paper, UV radiation resulted in the enhanced autophagy in HCE cells. Notably, the overexpression of miR-205-3p inhibited the autophagy level in HCE cells by regulating the expression of autophagy-related proteins, including reducing the expression of LC3II/I, ATG5, Berclin-1 and elevating P62 expression.

Inflammatory response and oxidative stress are two of the pathological features of damaged tissues. In this research, miR-205-3p was found to reduce the level of inflammatory factors in HCE cells exposed to UV radiation, such as TNF-α, IL-6 and IL-1β. In normal tissues, the generation and removal of ROS is in dynamic equilibrium. However, in damaged tissues, ROS was overproduced. As a response, a large amount of SOD and GSH-PX would be generated to remove the excessive ROS[21]. SOD and GSH-PX are two important defense factors against antioxidant damage[22,23]. Insufficient levels of SOD and GSH-PX led to the accumulation of ROS in tissues. The accumulated ROS attacked cell membrane and caused peroxidative damage of the cell lipid, which eventually led to the increased level of MDA (a marker of lipid peroxidation)[24-26]. This research revealed that ROS was elevated in HCE cells irradiated by UV. However, miR-205-3p could reduce ROS and elevate the level of SOD and GSH-PX in these damaged HCE cells.

At last, but not the least, through in-depth researches, we noticed that miR-205-3p might protect HCE cells from UV damage *via* regulating TLR4/NF-κB signaling. TLR4 had binding site for miR-205-3p, whose expression was directly suppressed by miR-205-3p. As early as 2009, Sun et al[27] have discovered that corneal inflammation could be inhibited by using antagonists of TLR4. In the cornea of mice infected with *Aspergillus fumigatus,* TLR4 was confirmed to be upregulated[28]. For rat infected by *Pseudomonas aeruginosa,* NLRP12 was reported to relieve corneal inflammation by downregulating the NF-κB signaling pathway[29]. Moreover, the inhibition of TLR4/NF-κB signaling pathway could attenuate autophagy and inflammatory injury of damaged tissues[30,31]. However, in corneal injury, especially UV-induced corneal damage, rare studies have investigated the effect of TLR4/NF-κB signaling on corneal damage. Our results pointed out for the first time that miR-205-3p could inhibit HCE cells from UV damage by suppressing the phosphorylation of NF-κB proteins *via* targeting TLR4.

Conclusions

Collectively, this paper explored for the first time that miR-205-3p protected HCE cells from UV damage by inhibiting autophagy *via* targeting TLR4/NF-κB signaling. MiR-205-3p might serve as an effective target for treating corneal damage caused by UV radiation. More researches would be implemented in the future in order to provide more favorable evidence and theoretical basis for this finding.

Conflict of Interest

The Authors declare that they have no conflict of interests.

Acknowledgements

This work is supported by Natural Science Foundation of Zhejiang Province (LGF18H120001), and Zhejiang Natural Science Foundation (LY20H120009).

References

1) Yu SL, Lee SK. Ultraviolet radiation: DNA damage, repair, and human disorders. Mol Cell Toxicol 2017; 13: 21-28.
2) Huang GQ, Yi GG, Wu LW, Feng SF, Wu W, Peng L, Yi RW, Ma W, Lu X. Protective effect of histatin 1 against ultraviolet-induced damage to human corneal epithelial cells. Exp Ther Med 2017; 15: 679-684.
3) Meeran SM, Punathil, Katiyar SK. IL-12 Deficiency exacerbates inflammatory responses in uv-irradiated skin and skin tumors. J Invest Dermatol 2008; 128: 2716-2727.
4) Kaplan N, Ventrella R, Peng H, Pal-Ghosh S, Arvanitis C, Rappoport JZ, Mitchell BJ, Stepp MA, Lavker RM, Getsios S. EphA2/Ephrin-A1 mediate corneal epithelial cell compartmentalization via ADAM10 regulation of EGFR signaling. Invest Ophthalmol Vis Sci 2018; 59: 393-406.
5) Bai WL, Dang YL, Yin RH, Yin RL, Jiang WQ, Wang ZY, Zhu YB, Wang JJ, Zhao ZH, Luo GB. Combination of let-7d-5p, miR-26a-5p, and miR-15a-5p is suitable normalizer for studying microRNA expression in skin tissue of Liaoning cashmere goat during hair follicle cycle. Czech J Anim Sci 2016; 61: 99-107.
6) Ratuszny D, Gras C, Bajor A, Börger AK, Pielen A, Börgel M, Framme C, Blasczyk R, Figueiredo C. MiR-145 is a promising therapeutic target to prevent cornea scarring. Hum Gene Ther 2015; 26: 698-707.
7) An J, Chen X, Chen W, Liang R, Reinach PS, Yan D, Tu L. MicroRNA expression profile and the role of miR-204 in corneal wound healing. Invest Ophthalmol Vis Sci 2015; 56: 3673-3683.

8) Seo M, Choi JS, Rho CR, Joo CK, Lee SK. MicroRNA miR-466 inhibits lymphangiogenesis by targeting prospero-related homeobox 1 in the alkali burn corneal injury model. J Biomed Sci 2015; 22: 3.

9) Lin D, Halilovic A, Yue P, Bellner L, Wang K, Wang L, Zhang C. Inhibition of miR-205 impairs the wound-healing process in human corneal epithelial cells by targeting KIR4.1 (KCNJ10). Invest Ophthalmol Vis Sci 2013; 54: 6167-6178.

10) Pennati M, Lopergolo A, Profumo V, De Cesare M, Sbarra S, Valdagni R, Zaffaroni N, Gandellini P, Folini M. MiR-205 impairs the autophagic flux and enhances cisplatin cytotoxicity in castration-resistant prostate cancer cells. Biochem Pharmacol 2014; 87: 579-597.

11) Wang W, Liu J, Wu Q. MiR-205 suppresses autophagy and enhances radiosensitivity of prostate cancer cells by targeting TP53INP1. Eur Rev Med Pharmacol Sci 2016; 20: 92-100.

12) Xu CG, Yang MF, Fan JX, Wang W. MiR-30a and miR-205 are downregulated in hypoxia and modulate radiosensitivity of prostate cancer cells by inhibiting autophagy via TP53INP1. Eur Rev Med Pharmacol Sci 2016; 20: 1501-1508.

13) Yang Y, Liu Y, Xue J, Yang Z, Shi Y, Shi Y, Lou G, Wu S, Qi J, Liu W, Wang J, Chen Z. MicroRNA-141 targets Sirt1 and inhibits autophagy to reduce HBV replication. Cell Physiol Biochem 2017; 41: 310-322.

14) Rittié L, Fisher GJ. UV-light-induced signal cascades and skin aging. Ageing Res Rev 2002; 1: 705-720.

15) Jiang M, Zhang P, Hu G, Xiao Z, Xu F, Zhong T, Huang F, Kuang H, Zhang W. Relative expressions of miR-205-5p, miR-205-3p, and miR-21 in tissues and serum of non-small cell lung cancer patients. Mol Cell Biochem 2013; 383: 67-75.

16) Andaur R, Tapia JC, Moreno J, Soto L, Armisen R, Marcelain K. Differential miRNA expression profiling reveals miR-205-3p to be a potential radiosensitizer for low-dose ionizing radiation in DLD-1 cells. Oncotarget 2018; 9: 26387-26405.

17) Asano J, Sato T, Ichinose S, Kajita M, Onai N, Shimizu S, Ohteki T. Intrinsic autophagy is required for the maintenance of intestinal stem cells and for irradiation-induced intestinal regeneration. Cell Rep 2017; 20: 1050-1060.

18) Laggner M, Pollreisz A, Schmidinger G, Schmidt-Erfurth U, Chen YT. Autophagy mediates cell cycle response by regulating nucleocytoplasmic transport of PAX6 in limbal stem cells under ultraviolet-A stress. PLoS One 2017; 12: e0180868.

19) Qiang L, Sample A, Shea CR, Soltani K, Macleod KF, He YY. Autophagy gene ATG7 regulates ultraviolet radiation-induced inflammation and skin tumorigenesis. Autophagy 2017; 137: 2086-2103.

20) Misovic M, Milenkovic D, Martinovic T, Ciric D, Bumbasirevic V, Kravic-Stevovic T. Short-term exposure to UV-A, UV-B, and UV-C irradiation induces alteration in cytoskeleton and autophagy in human keratinocytes. Ultrastruct Pathol 2013; 37: 241-248.

21) Zhou S, Sun Y, Zhuang Y, Zhao W, Chen Y, Jiang B, Guo C, Zhang Z, Peng H, Chen Y. Effects of kallistatin on oxidative stress and inflammation on renal ischemia-reperfusion injury in mice. Curr Vasc Pharmacol 2015; 13: 265-273.

22) Schneider MP, Sullivan JC, Wach PF, Boesen EI, Yamamoto T, Fukai T, Harrison DG, Pollock DM, Pollock JS. Protective role of extracellular superoxide dismutase in renal ischemia/reperfusion injury. Kidney Int 2010; 78: 374-381.

23) Wang J, Yang RW, Liu JB, Lin SY. Effects of soybean antioxidant peptides (SAP) on SOD, GSH-Px, CAT activity and MDA level in vivo. Advanced Materials Research, 2014; 1025-1026: 476-481.

24) Hu B, Wu Y, Tong F, Liu J, Shen X, Shen R, Xu G. Apocynin alleviates renal ischemia/reperfusion injury through regulating the level of zinc and metallothionen. Biol Trace Elem Res 2017; 178: 71-78.

25) Yusupov M, Wende K, Kupsch S, Neyts EC, Reuter S, Bogaerts A. Effect of head group and lipid tail oxidation in the cell membrane revealed through integrated simulations and experiments. Sci Rep 2017; 7: 5761.

26) Mendonça R, Gning O, Di Cesaré C, Lachat L, Bennett NC, Helfenstein F, Glauser G. Sensitive and selective quantification of free and total malondialdehyde in plasma using UHPLC-HRMS. J Lipid Res 2017; 58: 1924-1931.

27) Sun Y, Pearlman E. Inhibition of corneal inflammation by the TLR4 antagonist eritoran tetrasodium (E5564). Invest Ophthalmol Vis Sci 2009; 50: 1247-1254.

28) Liu M, Li C, Zhao GQ, Lin J, Che CY, Xu Q, Wang Q, Xu R, Niu YW. Boxb mediate BALB/c mice corneal inflammation through a TLR4/MyD88-dependent signaling pathway in Aspergillus fumigatus keratitis. Int J Ophthalmol 2018; 11: 548-552.

29) Deng QC, Deng CT, Li WS, Shu SW, Zhou MR, Kuang WB. NLRP12 promotes host resistance against Pseudomonas aeruginosa keratitis inflammatory responses through the negative regulation of NF-κB signaling. Eur Rev Med Pharmacol Sci 2018; 22: 8063-8075.

30) Feng Y, Cui Y, Gao JL, Li MH, Li R, Jiang XH, Tian YX, Wang KJ, Cui CM, Cui JZ. Resveratrol attenuates neuronal autophagy and inflammatory injury by inhibiting the TLR4/NF-κB signaling pathway in experimental traumatic brain injury. Int J Mol Med 2016; 37: 921-930.

31) Feng Y, Cui C, Liu X, Wu Q, Hu F, Zhang H, Ma Z, Wang L. Protective role of apocynin via suppression of neuronal autophagy and TLR4/NF-κB signaling pathway in a rat model of traumatic brain injury. Neurochem Res 2017; 42: 3296-3309.